Context-dependent functional substitution of α-skeletal actin by γ-cytoplasmic actin

Michele A. Jaeger,* Kevin J. Sonnemann,* Daniel P. Fitzsimons,† Kurt W. Prins,* and James M. Ervasti*,[1]

*Department of Biochemistry, Molecular Biology and Biophysics, University of Minnesota, Minneapolis, Minnesota, USA; and †Department of Physiology, University of Wisconsin, Madison, Wisconsin, USA

ABSTRACT **We generated transgenic mice that overexpressed γ-$_{cyto}$ actin 2000-fold above wild-type levels in skeletal muscle. γ-$_{cyto}$ actin comprised 40% of total actin in transgenic skeletal muscle, with a concomitant 40% decrease in α-actin. Surprisingly, transgenic muscle was histologically and ultrastructurally identical to wild-type muscle despite near-stoichiometric incorporation of γ-$_{cyto}$ actin into sarcomeric thin filaments. Furthermore, several parameters of muscle physiological performance in the transgenic animals were not different from wild type. Given these surprising results, we tested whether overexpression of γ-$_{cyto}$ actin could rescue the early postnatal lethality in α-$_{sk}$ actin-null mice (*Acta1*$^{-/-}$). By quantitative Western blot analysis, we found total actin levels were decreased by 35% in *Acta1*$^{-/-}$ muscle. Although transgenic overexpression of γ-$_{cyto}$ actin on the *Acta1*$^{-/-}$ background restored total actin levels to wild type, resulting in thin filaments composed of 60% γ-$_{cyto}$ actin and a 40% mixture of cardiac and vascular actin, the life span of transgenic *Acta1*$^{-/-}$ mice was not extended. These results indicate that sarcomeric thin filaments can accommodate substantial incorporation of γ-$_{cyto}$ actin without functional consequences, yet γ-$_{cyto}$ actin cannot fully substitute for α-$_{sk}$ actin.—Jaeger, M. A., Sonnemann, K. J., Fitzsimons, D. P., Prins, K. W., Ervasti, J. M. Context-dependent functional substitution of α-skeletal actin by γ-cytoplasmic actin. *FASEB J.* 23, 2205–2214 (2009)**

Key Words: isoforms · isoform substitution · myofibril · sarcomere · thin filament · nemaline myopathy

ACTIN IS ONE OF THE MOST abundant proteins in nature and is involved in a multitude of diverse cellular processes. Six unique actin isoforms exist within higher eukaryotes, each encoded by separate genes (1). Based on their predominant tissue-specific location, the actins are categorized into 4 muscle-specific isoforms [α-skeletal (α-$_{sk}$), α-cardiac (α-$_{ca}$), α-smooth (α-$_{sm}$), and γ-smooth (γ-$_{sm}$)] and 2 ubiquitously expressed isoforms [β-cytoplasmic (β-$_{cyto}$) and γ-cytoplasmic (γ-$_{cyto}$)]. The biological significance of multiple actin isoforms is not well understood, particularly since all 6 isoforms exhibit an extraordinary degree of amino acid sequence identity (>93%). However, several lines of evidence suggest that each isoform serves a unique purpose. First, all 6 actin isoforms are conserved from birds to mammals (2) and expressed in a tissue-specific and developmentally regulated manner (3, 4). Multiple actin isoforms also exist within an individual cell at specific ratios (4–7). In addition, actins are sorted into different subcellular compartments (4, 8–10), suggesting that cells can distinguish between isoforms.

Dramatic developmental shifts in actin isoform expression make skeletal muscle an ideal system for studying the role of multiple actins. Proliferating skeletal myoblasts almost exclusively express β- and γ-$_{cyto}$ actin, but on differentiation these cytoplasmic isoforms are drastically down-regulated and sequentially replaced by α-$_{ca}$ and α-$_{sm}$, and ultimately α-$_{sk}$ actin (11, 12). Although α-$_{sk}$ actin predominates in mature skeletal muscle, small amounts of other muscle and cytoplasmic actins remain. These actin populations sort to discrete areas of the muscle: sarcomeric actin (α-$_{ca}$ and α-$_{sk}$) to the thin filament and γ-$_{cyto}$ actin to the cortical actin cytoskeleton (13, 14). Although γ-$_{cyto}$ actin comprises only 1/4000 of the actin population (15), muscle-specific ablation of γ-$_{cyto}$ actin results in muscle that develops normally, but leads to a progressive myopathy (16).

Studies performed on cultured muscle cells have provided further evidence that cytoplasmic actin isoforms have distinct roles in muscle cells. Alteration of the normal 2:1 β- to γ-$_{cyto}$ actin ratio in myoblasts *via* overexpression of either cytoplasmic actin perturbed cellular morphology and cytoarchitecture (4). Moreover, transfection of cytoplasmic actins into adult cardiomyocytes resulted in deconstruction of the thin filament and cessation of spontaneous contractions, while transfection of muscle actins had no effect (17). Thus, *in vitro* studies suggest that perturbation of the native muscle actin population with cytoplasmic actins is detrimental to muscle cells.

To examine the effects of altering myocyte cytoplasmic actin populations *in vivo*, we generated transgenic

[1] Correspondence: Biochemistry, Molecular Biology, and Biophysics, University of Minnesota, 6-155 Jackson Hall, 321 Church St. SE, Minneapolis, MN 55455, USA. E-mail: jervasti@umn.edu

doi: 10.1096/fj.09-129783

mice that overexpressed γ-$_{cyto}$ actin specifically in skeletal muscle. Contrary to *in vitro* based predictions, >2000-fold overexpression of γ-$_{cyto}$ actin did not adversely affect skeletal muscle. Furthermore, γ-$_{cyto}$ actin incorporated into thin filaments without altering the functional performance of skeletal muscle. Given these surprising results, we addressed whether gross overexpression of γ-$_{cyto}$ actin rescued the postnatal lethality of α-$_{sk}$ actin-null mice (18). Despite a restoration of total actin to wild-type levels, expression of the γ-$_{cyto}$ actin transgene on the α-$_{sk}$ actin-null background was not able to rescue postnatal lethality, suggesting that γ-$_{cyto}$ actin cannot form functional thin filaments in skeletal muscle independent of α-$_{sk}$ actin. Our results demonstrate a context-dependent functional substitution of α-$_{sk}$ actin by γ-$_{cyto}$ actin.

MATERIALS AND METHODS

Generation of transgenic mice

The full coding sequence of the γ-$_{cyto}$ actin cDNA was reverse-transcribed from wild-type murine kidney RNA using the SuperScript OneStep RT-PCR with Platinum *Taq* kit (Invitrogen, Carlsbad, CA, USA) and primers KJS41 (5′-gatcgcaATGgaagaagaaatcgc-3′) and KJS42 (5′tgcctggcacctgctcagtc-3′). The *Actg1* 3′UTR was subsequently amplified using RT-PCR primers KJS45 (5′-cgaaatgcttctagatggactgag-3′) and KJS46 (5′-ttctttacacaatgacgtgttgctgg-3′) and cloned in frame with the coding sequence. This coding sequence-3′UTR construct was inserted downstream of the human skeletal α-actin (HSA) promoter and between the vp1 intron and tandem SV40 polyadenylation sequences of the HSAvpA expression cassette (kindly provided by Dr. Jeffrey Chamberlain, University of Washington, Seattle, WA, USA) to generate HSAcgaTg. The HSA promoter through the polyadenylation sequence fragment was excised from the plasmid backbone with *Cla*I/*Pvu*I digestion and microinjected into fertilized C57Bl/6 zygotes, which were then implanted into pseudopregnant female ICR mice. Resultant offspring were screened with transgene-specific primers KJS49 (5′-gtcacccacgtatgagtcttctgg-3′) and KJS51 (5′gaagcagacagtattcagcaagtaactg-3′) to identify mice carrying the transgene. Six founder mice were positively identified, and 4 of the 5 that survived to breeding age showed germline transmission and muscle-specific overexpression of γ-$_{cyto}$ actin. Transgenic line 3 mice showed the highest γ-$_{cyto}$ actin protein expression level and were used for all experiments. *Acta1*$^{+/-}$ male breeder mice were kindly provided by Dr. Nigel Laing and Dr. Kristen Nowak (University of Western Australia, Perth, Australia). Animals were housed and treated in accordance with the standards set by the institutional animal care and use committees at the University of Minnesota and University of Wisconsin.

Purification of bovine γ-$_{cyto}$ actin

The purification of γ-$_{cyto}$ actin from bovine brain was modified from Renley *et al.* (19). 125 g of unstripped mature bovine brain (Pel-Freeze Biologicals, Rogers, AR, USA) was cut into small pieces and placed in a cooled blender cup with 7 vol of G-buffer + protease inhibitors (2 mM Tris-HCl, 0.2 mM $CaCl_2$, 1 mM NaN_3, 0.1 mM ATP, 0.5 mM DTT, 0.1 mM benzamidine, 0.2 mM PMSF, 1.1 μM leupeptin, and 76 nM aprotinin, pH 7.5, at 4°C). The brain was homogenized on high speed (30 s on/ 30 s off, 3 times) and spun at 9000 *g* for 15 min. The resulting supernatant was spun at 125,000 *g* and filtered through 8 layers of cheesecloth. The supernatant was run over a column of 25 ml of DNase-I-Affi-Gel 10 and washed sequentially with 75 ml of G-buffer + protease inhibitors, 75 ml of 0.2 M NH_4Cl in G-buffer, and 75 ml of G-buffer. Actin was eluted off of the DNase-I-Affi-Gel 10 column and onto a 2-ml DEAE-Sepharose column with 60 ml of 30% deionized formamide in G-buffer. The DEAE-Sepharose column was then washed with 10 ml of G-buffer, and the actin was eluted with 18 1-ml fractions of 0.3 M KCl in G-buffer. Fractions containing actin (as determined by Coomassie gels and A280 readings) were pooled and stored at −80°C.

Determination of actin concentration in skeletal muscle

Known amounts of purified bovine brain actin or purified α-$_{sk}$ actin (purchased from Cytoskeleton, Denver, CO, USA) and known amounts of SDS extracts from *Actg1*-TG gastrocnemius or quadriceps femoris muscles were run side by side on a 3–12% SDS-polyacrylamide gel and transferred to nitrocellulose. Two γ-$_{cyto}$ actin antibodies (monoclonal mouse 2–4 and polyclonal affinity-purified rabbit 7577) were used for Western blotting, each at 1:1000 dilution. Two α-$_{sarc}$ actin antibodies were also used [monoclonal mouse 5c5 (Sigma, St. Louis, MO, USA) and monoclonal mouse Alpha-Sr-1 (Dako, Glostrup, Denmark)] at 1:1000 dilution. For blots comparing α-$_{sarc}$ actin levels between wild-type and *Actg1*-TG mice, fast skeletal myosin heavy chain (monoclonal mouse MY-32; Sigma) was used at a dilution of 1:1000 to adjust for equal loading between wild-type and *Actg1*-TG samples. To determine the concentration of actin (μg) in the SDS extracts, a concentration standard curve was derived from the known values of either purified bovine γ-$_{cyto}$ actin or purified α-$_{sk}$ actin using the densitometry and concentration standards feature on the Li-Cor software program (Li-Cor Biosciences, Lincoln, NE, USA).

Isolation of myofibrils

Strips of skeletal muscle were tied to small wooden dowels and soaked overnight at 4°C in 50% glycerol/50% wash solution (150 mM NaCl, 2 mM $MgCl_2$, 10 mM imidazole, 2 mM EGTA, 0.5 mM DTT, and 0.1 mM PMSF, pH 7.0). Muscles were then removed from the dowels, diced into small pieces with scissors, and incubated with stirring at 4°C for 30 min in 20 vol of cold wash buffer to remove glycerol. Fresh wash buffer (20 vol) was then added to the muscle, and it was homogenized on ice for 30 s with a Tissue Tearor homogenizer (Biospec Products, Bartlesville, OK, USA) on low setting. After centrifugation at 4000 *g* for 10 min, the pellet was washed by resuspending 3 times in 20 vol of wash buffer to remove cytoplasmic components, pelleting at 4000 *g* each time. The pellet was then resuspended and incubated for 20 min at 4°C in wash buffer containing 0.5% Triton X-100. After centrifugation at 4000 *g* for 10 min, the pellet was washed three more times with wash buffer, pelleting each time at 4000 *g* for 10 min. After the final wash and spin, the top white fluffy layer containing myofibrils was resuspended in wash buffer.

Confocal microscopy

Mouse skeletal muscle was dissected, frozen in melting isopentane, and mounted in O.C.T. medium (TissueTek, Torrance, CA, USA) for cryosectioning. Transverse sections (10 μm) of skeletal muscle were immediately fixed in 4% paraformaldehyde in PBS for 10 min, washed with PBS 3 × 2 min, and blocked with 5% goat serum in PBS for 30 min.

Primary antibody was diluted in PBS and applied to sections overnight at 4°C or at room temperature for 4 h. Sections were washed 3 × 2 min with PBS and secondary antibody (Alexa 488 and Alexa 568; Invitrogen) applied for 30 min at 37°C. After several washes with PBS, slides were coverslipped with a drop of ProLong Gold AntiFade with DAPI (Invitrogen). The following antibody dilutions were used for immunofluorescence experiments performed on transverse sections: 1:75 affinity purified γ-$_{cyto}$ actin rabbit 7577, 1:200 laminin α-2 rat clone 4H8–2 (Sigma) and 1:100 slow skeletal myosin clone NOQ7.5.4D (Sigma).

For immunofluorescence microscopy of isolated myofibrils, the myofibrils were diluted in ddH_2O and spread out to dry on Superfrost/Plus microscope slides (Fisher Scientific, Pittsburgh, PA, USA). The samples were then fixed, blocked, and stained as described above using the following dilutions: 1:75 affinity purified γ-$_{cyto}$ actin rabbit 7577, 1:100 fast myosin heavy chain clone MY-32 (Sigma), 1:500 α-actinin clone EA-53 (Sigma), 1:50 α-actin clone Sr-1 (Dako).

All images were obtained on an Olympus Fluoview 1000 Single Photon confocal microscope equipped with Olympus PlanApoN 1.42 NA ×60 oil, UPlanFL N 1.30 NA ×40 oil, and UPlan SApo 0.40 NA ×10 objective lenses (Olympus, Tokyo, Japan). Images were collected with Olympus Fluoview 1.7b software and assembled and processed with ImageJ (National Institutes of Health, Bethesda, MD, USA) and Adobe Photoshop (version 8.0; Adobe Systems, San Jose, CA, USA) software.

Serum creatine kinase analysis

Serum was collected and stored at −80°C until analysis. Serum (10 μl) was applied to a Vitros CK DT slide (Ortho-Clinical Diagnostics, Inc., Rochester, NY, USA) and analyzed with a Kodak Ektachem DT60 (Eastman Kodak Company, Rochester, NY, USA) and DTSE II module (Ortho-Clinical Diagnostics, Inc.).

Transmission electron microscopy

Anesthetized mice were transcardially perfused with 3% buffered glutaraldehyde, and desired muscles were excised and placed in glutaraldehyde for 2 additional hours. After extensive washing with 0.1 M PBS, samples were treated with 2% osmium tetroxide for 1 h, dehydrated in ethanol, and embedded in EMbed-812 (Electron Microscopy Sciences, Hatfield, PA, USA). Ultrathin sections were poststained with 5% uranyl acetate and 1% lead citrate and viewed on a Jeol 100CX transmission electron microscope (Jeol Ltd., Akishima, Japan).

Force measurements

Ex vivo force measurements

The extensor digitorum longus muscle from 4-mo-old mice was dissected; one tendon was attached to a rigid support and the other to a dual-mode servomotor. The muscle was allowed to equilibrate in a Ca^{2+}-Ringer's solution continuously gassed with 95% O_2/5% CO_2 to maintain a pH of 7.6 at 30°C. Platinum plate electrodes were positioned on either side of the muscle, and stimulation was induced by a single pulse lasting 200 μs. The muscle was adjusted to the length (L_0) at which maximal twitch force was achieved. The muscle was then subjected to an eccentric contraction regimen consisting of 5 maximal tetanic stimulations. Each stimulation was carried out over 700 ms; during the final 200 ms, the muscle was lengthened at a velocity of 0.5 L_0/s, resulting in a total stretch of 10% L_0.

In vivo physiological performance

Whole-body tension measurements were based on established techniques by Carlson and Makiejus (20). A mouse was attached by the tail to a horizontally mounted force transducer using suture silk and subsequently placed in an apparatus that allowed only forward movement. The force evoked by gentle tail pinches (~5 pinches/min) was recorded for 5 min, and the top 5 values were identified and normalized to body mass.

Maximal exercise performance was tested on a Columbus Instruments treadmill with an uphill grade of 15°(Columbus Instruments, Columbus, OH, USA). Mice were acclimated to the treadmill by running at a speed of 10 m/min for 5 min, 3 times/wk, for 2 wk. To determine maximal exercise performance mice were run on the treadmill for 5 min, at a speed of 10 m/min, followed by a 1-m/min increase in speed every minute until exhaustion. Mice were considered exhausted when they refused to stay off a shock bar for at least 5 s. Maximal exercise capacity was determined as the average duration of 2 trials separated by 2 d.

RESULTS

Actg1-TG mice overexpress γ-$_{cyto}$ actin >2000-fold in skeletal muscle

We used the HSA promoter to drive overexpression of the *Actg1* cDNA in murine skeletal muscle to examine how elevated levels of γ-$_{cyto}$ actin affect skeletal muscle *in vivo*. SDS lysates from transgenic γ-$_{cyto}$ actin (*Actg1*-TG) skeletal muscle were analyzed alongside a calibration curve of purified γ-$_{cyto}$ actin and quantified using the Li-Cor Odyssey infrared imaging system (**Fig. 1*A***). Quantitative Western blotting with 2 different γ-$_{cyto}$ actin antibodies (15) gave a value of 409 ± 43 μM γ-$_{cyto}$ actin in *Actg1*-TG skeletal muscle (Fig. 1*A*, *C*). In wild-type skeletal muscle, γ-$_{cyto}$ actin was previously measured at 0.197 ± 0.05 μM (15), but required extraction and enrichment in order to be measured. Thus, *Actg1*-TG mice minimally expressed γ-$_{cyto}$ actin at levels 2000-fold above wild type. Using the same methods, the abundance of α-sarcomeric actin (α-$_{sk}$ and α-$_{ca}$) was measured at 941 ± 123 μM for wild-type skeletal muscle (Fig. 1*B*), which is very similar to the 893 ± 42 μM α-$_{sarc}$ actin reported previously for wild-type skeletal muscle (15). In *Actg1*-TG skeletal muscle, α-$_{sarc}$ actin abundance was measured at 571 ± 51 μM (Fig. 1*A*, *C*). Together, γ-$_{cyto}$ actin (409 μM) and α-$_{sarc}$ actin (571 μM) levels in *Actg1*-TG skeletal muscle totaled 980 μM, which is consistent with α-$_{sarc}$ actin abundance in wild-type muscle (941 μM) (Fig. 1*C*). Thus, up-regulation of γ-$_{cyto}$ actin in *Actg1*-TG skeletal muscle led to a concomitant down-regulation of α-$_{sarc}$ actin to maintain total actin levels similar to α-$_{sarc}$ actin abundance in wild-type muscle.

γ-$_{cyto}$ actin incorporates into *Actg1*-TG thin filaments

To determine the localization of γ-$_{cyto}$ actin in *Actg1*-TG mice, immunofluorescence microscopy was performed

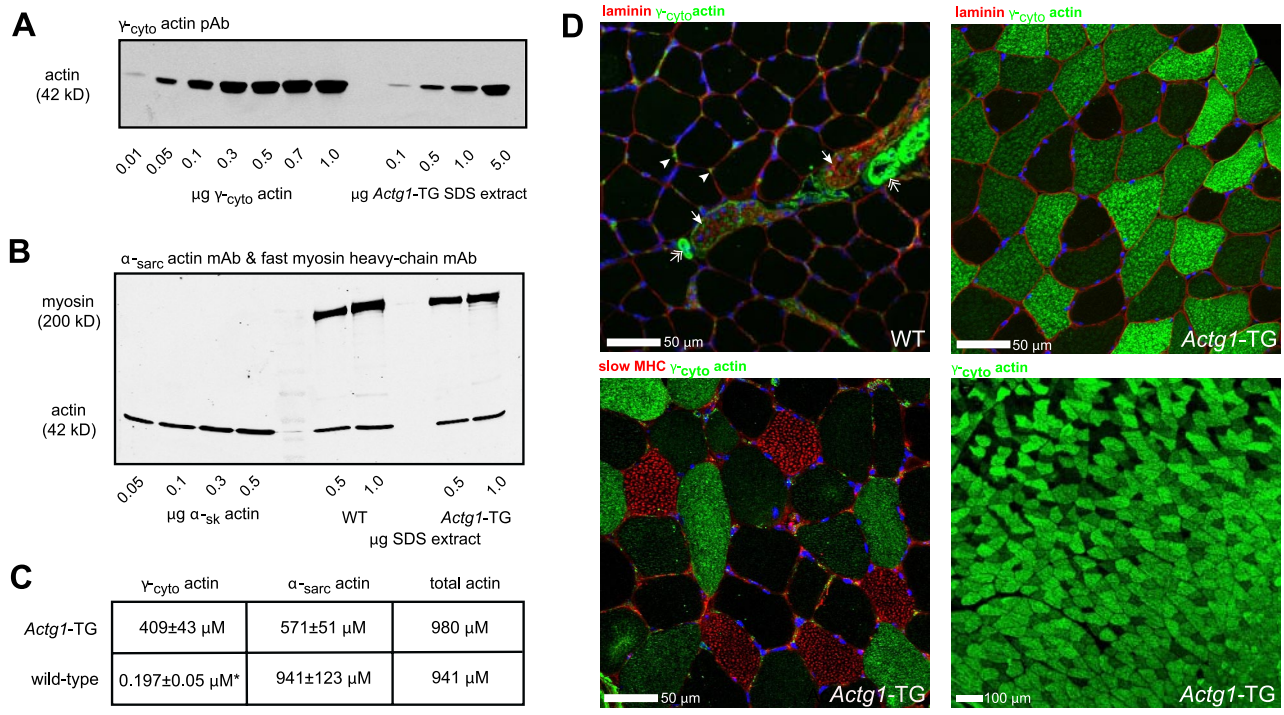

Figure 1. *Actg1*-TG mice express γ-$_{cyto}$ actin 2000-fold above wild-type levels in skeletal muscle. *A, B*) Quantitative Western blot analysis was performed to determine the concentration of γ-$_{cyto}$ actin (*A*) and α-$_{sarc}$ actin (*B*) in skeletal muscle. *C*) *Actg1*-TG mice expressed γ-$_{cyto}$ actin in skeletal muscle at levels that were >2000-fold above wild-type levels. However, total actin levels were not altered due to decreased α-$_{sarc}$ actin expression in skeletal muscle. *Wild-type skeletal muscle α-$_{sarc}$ actin levels previously calculated (15). *D*) γ-$_{Cyto}$ actin staining was predominately seen in capillaries (arrowhead), blood vessels (double-headed arrow) and nerves (arrow) in wild-type skeletal muscle. In addition, γ-$_{cyto}$ actin brightly stained the internal structure of fast-twitch fibers in *Actg1*-TG skeletal muscle.

on transverse cryosections of wild-type and *Actg1*-TG muscles. In wild-type skeletal muscle, γ-$_{cyto}$ actin polyclonal antibodies brightly stained capillaries, blood vessels and nerves (Fig. 1*D*). No internal staining was observed in wild-type myofibers. However, the internal space of many *Actg1*-TG fibers stained intensely, while some smaller fibers were devoid of staining (Fig. 1*D*). Staining with slow myosin heavy chain and γ-$_{cyto}$ actin antibody demonstrated that many fibers devoid of staining were slow-twitch fibers, although not exclusively. This staining pattern was consistent with reports that the HSA promoter is preferentially expressed in fast-twitch myofibers (21). Staining of gastrocnemius, quadriceps femoris, tibialis anterior, extensor digitorum longus, and diaphragm with γ-$_{cyto}$ actin antibody showed that >90% of the fibers within each muscle had medium to high-intensity staining. Fibers that showed little to no γ-$_{cyto}$ actin expression tended to cluster in focal areas of muscle, whereas other larger regions showed homogenous bright staining (see gastrocnemius staining in lower right panel of Fig. 1*D*).

The internal space of muscle fibers is comprised of a densely packed network of myofibrils. Myofibrils are composed of repeating thick- and thin-filament bundles that make up the contractile sarcomere. Normally, α-$_{sk}$ actin is the dominant, if not sole, actin isoform within sarcomeric thin filaments of adult skeletal muscle. To determine whether the intense γ-$_{cyto}$ actin staining present in *Actg1*-TG muscle resulted from γ-$_{cyto}$ actin incorporation into thin filaments, immunostaining was performed on isolated myofibrils. Bright staining of γ-$_{cyto}$ actin was observed interspersed between thick filaments in *Actg1*-TG myofibrils (as indicated by fast myosin heavy chain staining, **Fig. 2*A***), but was absent in wild-type myofibrils. Also consistent with thin-filament incorporation, γ-$_{cyto}$ actin staining flanked α-actinin Z-disk staining (Fig. 2*B*). Myofibrils probed with both α-$_{sarc}$ actin and γ-$_{cyto}$ actin showed areas of colocalization (Fig. 2*C*). However, some areas showed differential enrichment of either γ-$_{cyto}$ actin or α-$_{sarc}$ actin (Fig. 2*C*). Combined, these immunofluorescence analyses demonstrate that γ-$_{cyto}$ actin in *Actg1*-TG mice localized to areas that are consistent with incorporation into thin filaments.

Gross overexpression of γ-$_{cyto}$ actin does not adversely affect muscle cell architecture or integrity *in vivo*

Based on the detrimental effects of overexpressing γ-$_{cyto}$ actin *in vitro* (4, 17, 22), we examined *Actg1*-TG mice for evidence of muscle pathology. Transmission electron microscopy of *Actg1*-TG skeletal muscle revealed well-defined sarcomeres and overall ultrastructure that was indistinguishable from wild-type skeletal muscle (**Fig. 3*A***). Hematoxylin and eosin (H&E)-stained transverse cryosections of *Actg1*-TG skeletal

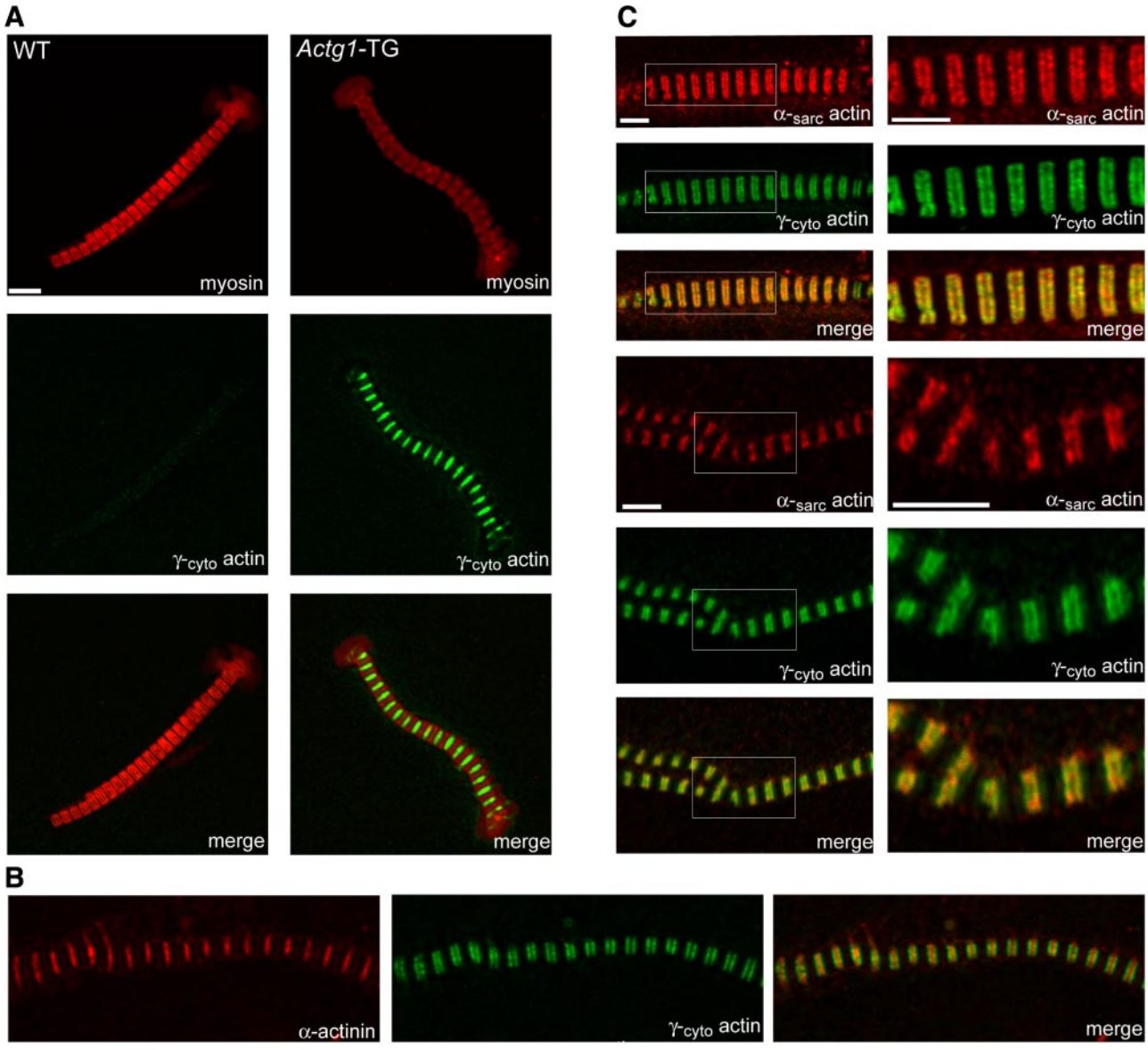

Figure 2. γ-$_{cyto}$ actin incorporates into *Actg1*-TG skeletal muscle thin filaments. *A*) Isolated myofibrils from wild-type or *Actg1*-TG mice were stained with γ-$_{cyto}$ actin and fast myosin heavy chain. *B, C*) *Actg1*-TG isolated myofibrils were stained with γ-$_{cyto}$ actin and α-actinin or α-$_{sarc}$ actin. Boxed areas in left panels of *C* are magnified at right. Scale bars = 5 μm.

muscle also demonstrated that the general fiber architecture (shape and size) was similar to wild-type skeletal muscle (Fig. 3*B*). In addition, no fibrosis, fat deposits, or mononuclear cell infiltration were observed. To quantitatively assess whether gross overexpression of γ-$_{cyto}$ actin in muscle resulted in muscle pathology, levels of centrally nucleated fibers (CNFs) in H&E-stained tibialis anterior and gastrocnemius muscle were quantified from wild-type, *Actg1*-TG, and dystrophin-deficient *mdx* mice. Muscle nuclei are normally located at the periphery of myofibers; however, the nuclei are located internally in a cell that has been damaged and subsequently regenerated. In *Actg1*-TG tibialis anterior and gastrocnemius muscles, CNF levels were very low ($<$2% at all ages) and not significantly different from wild type (Fig. 3*C*). In contrast, the *mdx* mouse exhibited $>$30% CNF in each muscle at all ages examined (Fig. 3*C*). In addition to histological parameters, many mouse models of muscle disease exhibit high serum levels of the muscle enzyme creatine kinase, indicative of sarcolemmal damage. *Actg1*-TG mice had wild-type serum creatine kinase levels, while *mdx* mice had significantly higher serum creatine kinase levels (Fig. 3*C*). Overall, *Actg1*-TG skeletal muscle had normal cytoarchitecture with no evidence of increased cell death or membrane damage.

Actg1-TG mice exhibit normal *ex vivo* and *in vivo* muscle performance

Because perturbation of the actin composition in cardiac muscle thin filaments altered cardiac muscle contractile properties (23), a series of *in vivo* and *ex vivo* force measurements were performed with *Actg1*-TG

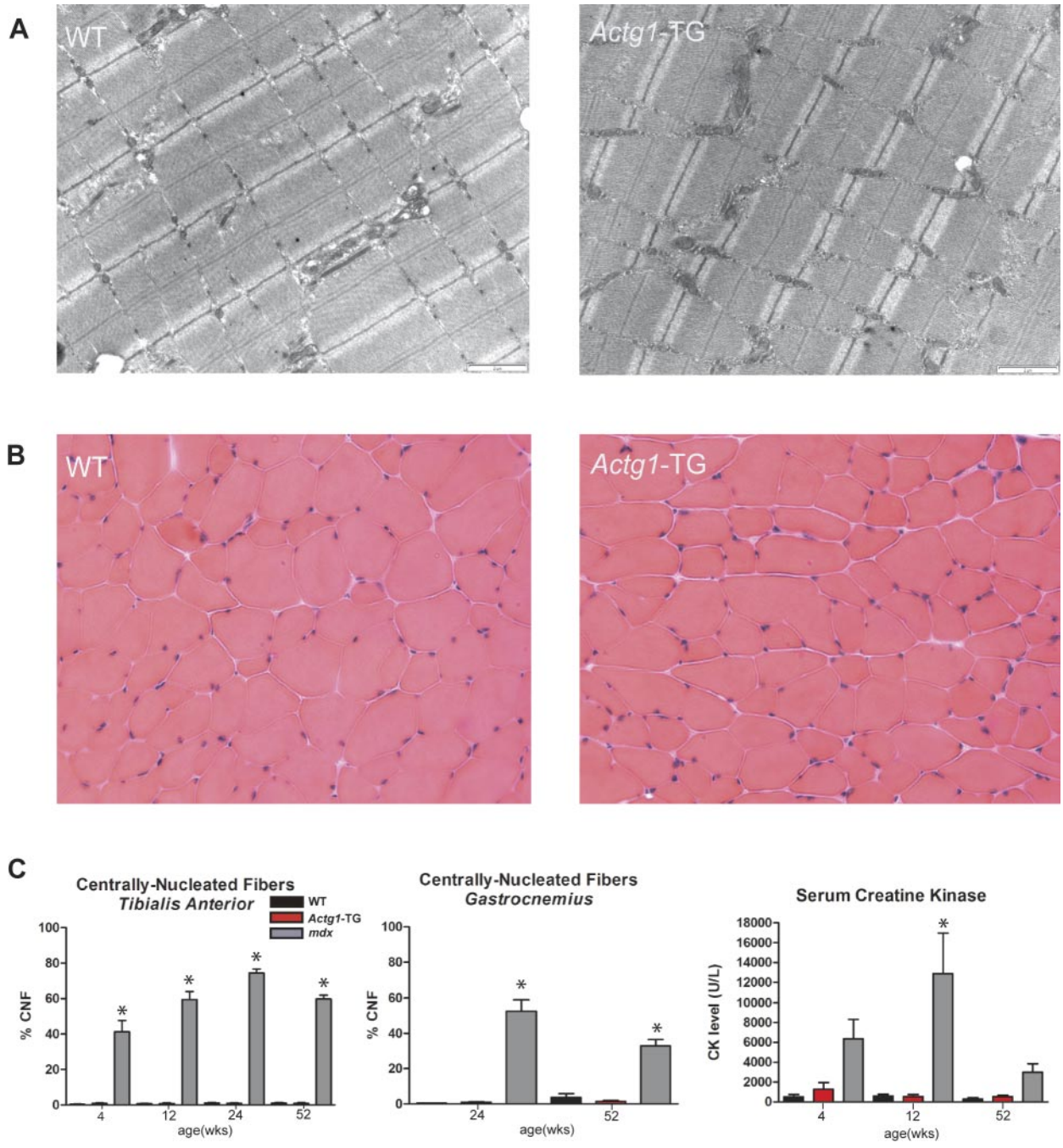

Figure 3. Gross overexpression of γ-$_{cyto}$ actin in skeletal muscle does not result in muscle pathology. *A*) Transmission electron micrographs of 2-mo-old wild-type and *Actg1*-TG gastrocnemius muscle. No ultrastructural abnormalities were observed in *Actg1*-TG samples. Scale bars = 2 μm. *B*) H&E-stained cryosections from 1-yr-old wild-type and *Actg1*-TG gastrocnemius muscle. *C*) CNFs were quantified from entire H&E sections of tibialis anterior and gastrocnemius muscles at various time points. Both wild-type and *Actg1*-TG muscles had low levels of CNFs, as well as low levels of serum creatine kinase, compared to the myopathic *mdx* mouse model. $*P < 0.05$ *vs.*wild-type and *Actg1*-TG samples; 1-way ANOVA with Tukey's multiple comparison *post hoc* test; $n \geq 3$ for each genotype/time point. Error bars = SEM.

mice to determine whether incorporation of γ-$_{cyto}$ actin into sarcomeres affected muscle performance. *Ex vivo* analyses were conducted on isolated extensor digitorum longus muscles, which expressed high levels of γ-$_{cyto}$ actin (**Fig. 4*A***). Twitch force—the amount of force elicited by a single action potential—was identical between wild-type and *Actg1*-TG muscle (Fig. 4*A*). Similarly, the maximal force generated during tetanic stimulation was indistinguishable between the 2 groups (Fig. 4*A*). Force generation following a series of eccentric (lengthening) contractions was also examined. While eccentric contractions are injurious to even wild-type muscle, several animal models of muscular dystrophy display significantly greater susceptibility to eccentric contraction induced muscle damage (24–27). *Actg1*-TG and wild-type extensor digitorum longus mus-

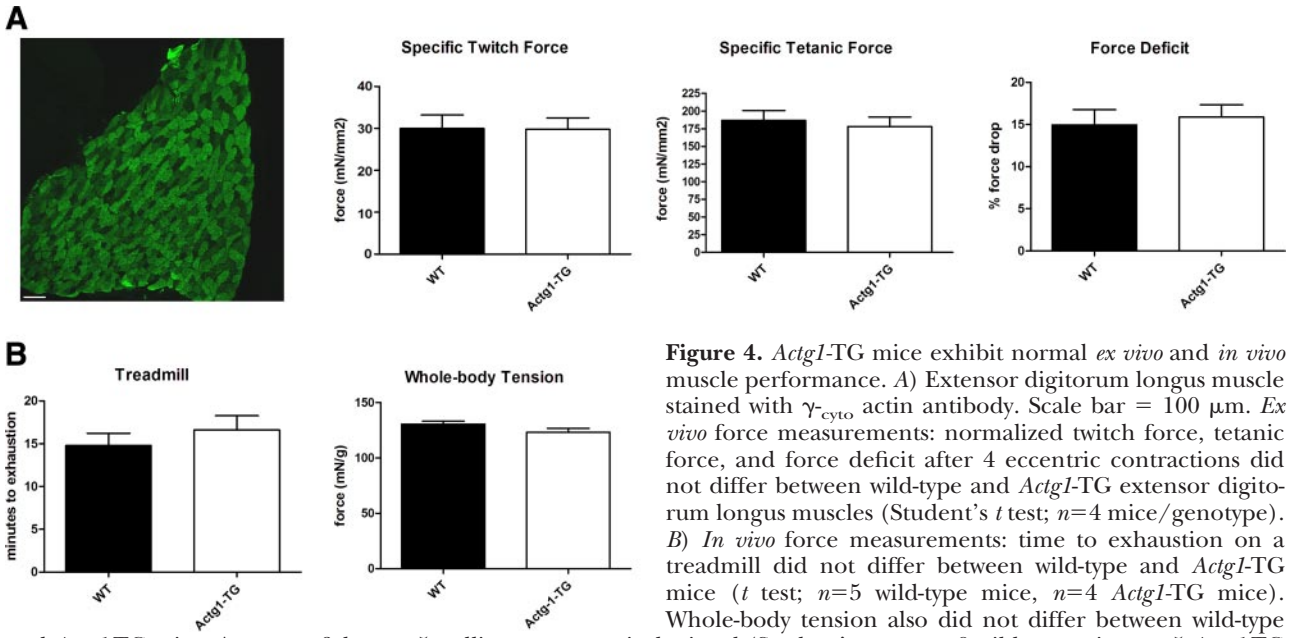

Figure 4. *Actg1*-TG mice exhibit normal *ex vivo* and *in vivo* muscle performance. *A*) Extensor digitorum longus muscle stained with γ-$_{cyto}$ actin antibody. Scale bar = 100 μm. *Ex vivo* force measurements: normalized twitch force, tetanic force, and force deficit after 4 eccentric contractions did not differ between wild-type and *Actg1*-TG extensor digitorum longus muscles (Student's *t* test; n=4 mice/genotype). *B*) *In vivo* force measurements: time to exhaustion on a treadmill did not differ between wild-type and *Actg1*-TG mice (*t* test; n=5 wild-type mice, n=4 *Actg1*-TG mice). Whole-body tension also did not differ between wild-type and *Actg1*-TG mice. Average of the top 5 pulling responses is depicted (Student's *t* test; n=9 wild-type mice, n=5 *Actg1*-TG mice). Error bars = SEM.

cles showed a similar decrement in maximal force production after four eccentric contractions (Fig. 4*A*). Similarly, *in vivo* studies examining treadmill endurance and whole-body force generation showed no differences between wild-type and *Actg1*-TG mice (Fig. 4*B*). Overall, thin filaments composed of 40% γ-$_{cyto}$ actin were functionally equivalent to wild-type filaments.

Gross overexpression of γ-$_{cyto}$ does not rescue α-$_{sk}$ actin-null mouse lethality

As sarcomeres containing near-stoichiometric amounts of γ-$_{cyto}$ actin were fully functional (Fig. 4), we tested the hypothesis that overexpression of γ-$_{cyto}$ actin in skeletal muscle could rescue the postnatal lethality associated with the absence of α-$_{sk}$ actin. Mice null for α-$_{sk}$ actin (*Acta1*$^{-/-}$) are indistinguishable from their littermates at birth but die by postnatal day 10 (18). Similarly, humans born without α-$_{sk}$ actin are severely impaired and often die within the first few months of life (28). We crossed *Acta1*$^{+/-}$ with *Actg1*-TG mice to generate mice that were null for α-$_{sk}$ actin and overexpressed γ-$_{cyto}$ actin in skeletal muscle (*Acta1*$^{-/-}$;TG). Both *Acta1*$^{-/-}$ and *Acta1*$^{-/-}$;TG mice were born at expected Mendelian ratios (**Fig. 5*A***). Interestingly, in the absence of α-$_{sk}$ actin, *Acta1*$^{-/-}$*;TG* mice expressed γ-$_{cyto}$ actin at significantly higher levels (631 μM) than *Actg1*-TG mice (409 μM) (Fig. 5*B*), indicating that transgene expression was context dependent. Although *Acta1*$^{-/-}$ mice are able to form skeletal muscle *via* the up-regulation of α-$_{ca}$ and α-$_{sm}$ actin (18), quantitative Western blotting of total muscle extracts with a pan-actin antibody revealed that *Acta1*$^{-/-}$ skeletal muscle contained 35% less actin than wild-type skeletal muscle (Fig. 5*C*). Total actin levels were restored when the *Actg1* transgene was expressed on the *Acta1*$^{-/-}$ background (Fig. 5*C*). Despite wild-type levels of actin, *Acta1*$^{-/-}$;TG mice did not thrive. Similar to *Acta1*$^{-/-}$ pups, *Acta1*$^{-/-}$;TG pups failed to gain weight normally (Fig. 5*D*), were smaller in stature than their littermates (Fig. 5*E*), and died by 15 d of age (Fig. 5*F*). *Acta1*$^{-/-}$;TG skeletal muscle was histologically indistinguishable from *Acta1*$^{-/-}$ skeletal muscle (data not shown), displaying prominent interstitial space between fibers, as described previously (18). Collectively, these results indicate that, while γ-$_{cyto}$ actin can contribute to functional thin filaments in the presence of α-$_{sk}$ actin, γ-$_{cyto}$ actin cannot serve as a functional replacement for α-$_{sk}$ actin.

DISCUSSION

We examined whether a cytoplasmic actin can function as a muscle actin *in vivo* by transgenically overexpressing γ-$_{cyto}$ actin in skeletal muscle and observed that γ-$_{cyto}$ actin can form functional thin filaments in a context-dependent manner. A 2000-fold up-regulation of γ-$_{cyto}$ actin and corresponding decrease in α-$_{sarc}$ actin resulted in γ-$_{cyto}$ actin representing nearly 50% of the total actin population in transgenic skeletal muscle. The maintenance of total actin at wild-type levels supports previous observations that sarcomeric protein levels are maintained at strict stoichiometries (29–32). We also observed that γ-$_{cyto}$ actin incorporated efficiently into myofibrillar thin filaments, which agrees with most *in vitro* studies (33, 34). Although von Arx *et al.* (17) reported that γ-$_{cyto}$ actin overexpression dramatically perturbed the cytoarchitecture and contractile function of cardiac myocytes, our results demonstrate that γ-$_{cyto}$ actin is capable of near stoichiomet-

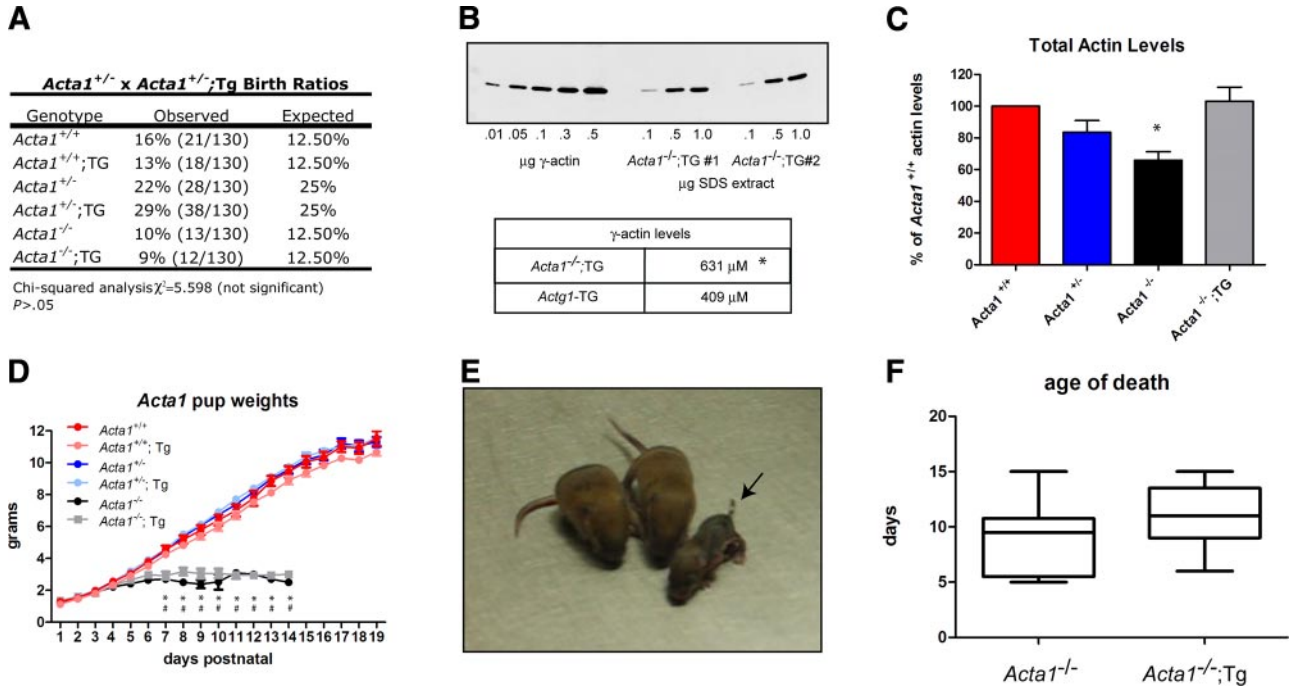

Figure 5. Transgenic γ-$_{cyto}$ actin overexpression cannot rescue *Acta1*$^{-/-}$ lethality. *A*) All pups were born at expected Mendelian ratios as determined by χ^2 analysis. *B*) γ-$_{Cyto}$ actin levels were significantly higher in *Acta1*$^{-/-}$;TG skeletal muscle compared to adult *Actg1*-TG skeletal muscle. **P* = 0.0007; unpaired *t* test. *C*) Total actin abundance was significantly lower in *Acta1*$^{-/-}$ skeletal muscle compared to wild-type skeletal muscle. However, total actin abundance was restored with transgenic overexpression of γ-$_{cyto}$ actin. **P* < 0.0001 *vs.* *Acta1*$^{+/+}$; single-sample 2-tailed *t* test. *D*) *Acta1*$^{-/-}$ and *Acta1*$^{-/-}$;TG pups weighed significantly less than their littermates from 7 d of age until their natural death. **P* < 0.01, *Acta1*$^{-/-}$;TG *vs.* *Acta1*$^{+/+}$; $^{\#}$*P* < 0.01, *Acta1*$^{-/-}$ *vs.* *Acta1*$^{+/+}$; 2-way ANOVA. *E*) *Acta1*$^{-/-}$ and *Acta1*$^{-/-}$;TG mice were smaller in stature compared to littermates. Representative image of an *Acta1*$^{-/-}$;TG pup at 11 d of age (arrow). *F*) Age of death did not differ significantly between *Acta1*$^{-/-}$ and *Acta1*$^{-/-}$;TG mice. *P* > 0.05; paired *t* test.

ric incorporation into skeletal myofibrils *in vivo* without disrupting skeletal muscle cytoarchitecture or function.

Actg1-TG muscle performance was identical to wild type as measured through several *ex vivo* and *in vivo* assays, suggesting that there is considerable functional redundancy between γ-$_{cyto}$ and α-$_{sk}$ actin isoforms. Therefore, we tested whether γ-$_{cyto}$ actin overexpression could rescue the early postnatal lethality associated with total α-$_{sk}$ actin deficiency. *Acta1*$^{-/-}$ mice can breathe, suckle, and walk at birth (18). Although *Acta1*$^{-/-}$ skeletal muscle up-regulates alternative actin isoforms (α-$_{ca}$, α-$_{sm}$, and γ-$_{sm}$) and exhibits no obvious ultrastructural defects, mice fail to gain weight, have weaker muscles, and die by 10 d of age (18). We measured the total actin abundance in *Acta1*$^{-/-}$ skeletal muscle and found that it was significantly lower (35%) than in wild-type mice. We also noted that *Acta1*$^{+/-}$ skeletal muscle expressed 17% less actin (Fig. 5*C*), but heterozygous mice did not present with an overt phenotype (ref. 18 and unpublished results). Although γ-$_{cyto}$ actin overexpression restored total muscle actin to wild-type levels, the *Actg1* transgene was not able to significantly prolong survival in *Acta1*$^{-/-}$ pups. From these data, we conclude that thin-filament actin isoform composition—and not concentration—is critical for normal skeletal muscle function. Similar results were observed in *Drosophila melanogaster*, whereby complete replacement of flight muscle actin with cytoplasmic actin resulted in disruption of flight muscle structure and function (35).

In contrast to our data, transgenic overexpression of α-$_{ca}$ actin fully rescued *Acta1*$^{-/-}$ mice (36), supporting the observation that survival beyond birth in *ACTA1*-null humans correlates with the extent of α-$_{ca}$ actin up-regulation (28). Similarly, transgenic overexpression of γ-$_{sm}$ actin rescued α-$_{ca}$ actin-mice from embryonic and postnatal lethality (37). In both α-$_{sk}$- and α-$_{ca}$-null mice, up-regulation of alternative actin isoforms resulted in the formation of sarcomeric structures. However, transgenic overexpression of distinct muscle actin isoforms was necessary to rescue lethality, arguing that a threshold level of muscle actin expression is necessary for viability. In all cases where transgenic or endogenous up-regulation of a muscle actin compensated for a muscle actin deficiency the muscle was functionally distinct from wild type (36–38), arguing that muscle actins are optimally suited for their respective tissue-specific functions.

Our results extend the prior studies by demonstrating that thin filaments composed of 40% γ-$_{cyto}$ actin retain wild-type function, yet thin filaments composed of 60% γ-$_{cyto}$ actin in the absence of α-$_{sk}$ actin result in nonviable mice. The former result is surprising given that actin isoforms show different efficiencies in activating skeletal muscle myosin ATPase (39–42) and overexpression of γ-$_{sm}$ actin in wild-type hearts altered

contractile performance (23). We can envision several scenarios that may explain our current results. First, at 40% incorporation of $\gamma\text{-}_{cyto}$ actin into *Acta1*$^{+/+}$ sarcomeres, each $\gamma\text{-}_{cyto}$ actin molecule would likely be adjacent to an $\alpha\text{-}_{sk}$ actin molecule, which may allosterically influence $\gamma\text{-}_{cyto}$ actin molecules to behave like $\alpha\text{-}_{sk}$ actin subunits. At a higher molar ratio such as that measured in the *Acta1*$^{-/-}$;TG skeletal muscle (60%), $\gamma\text{-}_{cyto}$ actin molecules bounded by identical neighbors may function as cytoskeletal filaments with altered structure or dynamics that no longer properly support skeletal myosin or thin-filament regulatory protein function. Alternatively, the combined up-regulation of $\gamma\text{-}_{cyto}$, $\alpha\text{-}_{ca}$, $\alpha\text{-}_{sm}$, and $\gamma\text{-}_{sm}$ isoforms in *Acta1*$^{-/-}$;TG skeletal muscle may yield sarcomeric thin filaments that are simply too heterogeneous to sustain normal muscle function. Yet a third possibility is that there may be an unidentified function for $\alpha\text{-}_{sk}$ actin that is independent of muscle contraction, perhaps outside of the thin-filament compartment.

The functional significance behind the strict conservation of actin coding sequences throughout evolution remains elusive. Our data indicate that partial substitution of one actin isoform for another without functional consequences is insufficient to conclude there is complete functional redundancy. Therefore, the development of new mouse "rescue" models designed to investigate functional redundancy among actin family members in a tissue-specific context is currently the most logical route to answer such questions. In addition, future studies to identify how isoform substitution influences the expression or function of actin regulatory proteins are likely required before we can adequately understand the importance and significance of the 6 highly conserved, yet functionally distinct actin isoforms. FJ

The authors thank Dr. Nigel Laing and Dr. Kristen Nowak (University of Western Australia, Perth, Australia) for generously providing *Acta1*$^{+/-}$ mice and for sharing their data prior to publication, and Dr. Richard L. Moss for helpful comments and suggestions. This study was supported by American Heart Association Predoctoral Fellowships to M.A.J and K.J.S., and NIH grant AR049899 to J.M.E.

REFERENCES

1. Firtel, R. A. (1981) Multigene families encoding actin and tubulin. *Cell* **24,** 6–7
2. Rubenstein, P. A. (1990) The functional importance of multiple actin isoforms. *Bioessays* **12,** 309–315
3. McHugh, K. M., Crawford, K., and Lessard, J. L. (1991) A comprehensive analysis of the developmental and tissue-specific expression of the isoactin multigene family in the rat. *Dev. Biol.* **148,** 442–458
4. Schevzov, G., Lloyd, C., and Gunning, P. (1992) High level expression of transfected beta- and gamma-actin genes differentially impacts on myoblast cytoarchitecture. *J. Cell Biol.* **117,** 775–785
5. Erba, H. P., Eddy, R., Shows, T., Kedes, L., and Gunning, P. (1988) Structure, chromosome location, and expression of the human gamma-actin gene: differential evolution, location, and expression of the cytoskeletal beta- and gamma-actin genes. *Mol. Cell. Biol.* **8,** 1775–1789
6. Bravo, R., Fey, S. J., Small, J. V., Larsen, P. M., and Celis, J. E. (1981) Coexistence of three major isoactins in a single sarcoma 180 cell. *Cell.* **25,** 195–202
7. Otey, C. A., Kalnoski, M. H., and Bulinski, J. C. (1987) Identification and quantification of actin isoforms in vertebrate cells and tissues. *J. Cell. Biochem.* **34,** 113–124
8. DeNofrio, D., Hoock, T. C., and Herman, I. M. (1989) Functional sorting of actin isoforms in microvascular pericytes. *J. Cell Biol.* **109,** 191–202
9. Otey, C. A., Kalnoski, M. H., and Bulinski, J. C. (1988) Immunolocalization of muscle and nonmuscle isoforms of actin in myogenic cells and adult skeletal muscle. *Cell Motil. Cytoskeleton* **9,** 337–348
10. Pardo, J. V., Pittenger, M. F., and Craig, S. W. (1983) Subcellular sorting of isoactins: selective association of gamma actin with skeletal muscle mitochondria. *Cell* **32,** 1093–1103
11. Bains, W., Ponte, P., Blau, H., and Kedes, L. (1984) Cardiac actin is the major actin gene product in skeletal muscle cell differentiation in vitro. *Mol. Cell. Biol.* **4,** 1449–1453
12. Gunning, P., Hardeman, E., Wade, R., Ponte, P., Bains, W., Blau, H. M., and Kedes, L. (1987) Differential patterns of transcript accumulation during human myogenesis. *Mol. Cell. Biol.* **7,** 4100–4114
13. Rybakova, I. N., Patel, J. R., and Ervasti, J. M. (2000) The dystrophin complex forms a mechanically strong link between the sarcolemma and costameric actin. *J. Cell Biol.* **150,** 1209–1214
14. Craig, S. W., and Pardo, J. V. (1983) Gamma actin, spectrin, and intermediate filament proteins colocalize with vinculin at costameres, myofibril-to-sarcolemma attachment sites. *Cell Motil.* **3,** 449–462
15. Hanft, L. M., Rybakova, I. N., Patel, J. R., Rafael-Fortney, J. A., and Ervasti, J. M. (2006) Cytoplasmic gamma-actin contributes to a compensatory remodeling response in dystrophin-deficient muscle. *Proc. Natl. Acad. Sci. U. S. A.* **103,** 5385–5390
16. Sonnemann, K. J., Fitzsimons, D. P., Patel, J. R., Liu, Y., Schneider, M. F., Moss, R. L., and Ervasti, J. M. (2006) Cytoplasmic gamma-actin is not required for skeletal muscle development but its absence leads to a progressive myopathy. *Dev. Cell.* **11,** 387–397
17. von Arx, P., Bantle, S., Soldati, T., and Perriard, J. C. (1995) Dominant negative effect of cytoplasmic actin isoproteins on cardiomyocyte cytoarchitecture and function. *J. Cell Biol.* **131,** 1759–1773
18. Crawford, K., Flick, R., Close, L., Shelly, D., Paul, R., Bove, K., Kumar, A., and Lessard, J. (2002) Mice lacking skeletal muscle actin show reduced muscle strength and growth deficits and die during the neonatal period. *Mol. Cell. Biol.* **22,** 5887–5896
19. Renley, B. A., Rybakova, I. N., Amann, K. J., and Ervasti, J. M. (1998) Dystrophin binding to nonmuscle actin. *Cell. Motil. Cytoskeleton* **41,** 264–270
20. Carlson, C. G., and Makiejus, R. V. (1990) A noninvasive procedure to detect muscle weakness in the mdx mouse. *Muscle Nerve* **13,** 480–484
21. Tinsley, J. M., Potter, A. C., Phelps, S. R., Fisher, R., Trickett, J. I., and Davies, K. E. (1996) Amelioration of the dystrophic phenotype of mdx mice using a truncated utrophin transgene. *Nature* **384,** 349–353
22. Lloyd, C. M., Berendse, M., Lloyd, D. G., Schevzov, G., and Grounds, M. D. (2004) A novel role for non-muscle gamma-actin in skeletal muscle sarcomere assembly. *Exp. Cell. Res.* **297,** 82–96
23. Martin, A. F., Phillips, R. M., Kumar, A., Crawford, K., Abbas, Z., Lessard, J. L., de Tombe, P., and Solaro, R. J. (2002) Ca(2+) activation and tension cost in myofilaments from mouse hearts ectopically expressing enteric gamma-actin. *Am. J. Physiol. Heart. Circ. Physiol.* **283,** H642–649
24. Moens, P., Baatsen, P. H., and Marechal, G. (1993) Increased susceptibility of EDL muscles from mdx mice to damage induced by contractions with stretch. *J. Muscle. Res. Cell. Motil.* **14,** 446–451
25. Petrof, B. J., Shrager, J. B., Stedman, H. H., Kelly, A. M., and Sweeney, H. L. (1993) Dystrophin protects the sarcolemma from stresses developed during muscle contraction. *Proc. Natl. Acad. Sci. U. S. A.* **90,** 3710–3714

26. Barton, E. R. (2006) Impact of sarcoglycan complex on mechanical signal transduction in murine skeletal muscle. *Am. J. Physiol. Cell. Physiol.* **290,** C411–C419
27. Hack, A. A., Lam, M. Y., Cordier, L., Shoturma, D. I., Ly, C. T., Hadhazy, M. A., Hadhazy, M. R., Sweeney, H. L., and McNally, E. M. (2000) Differential requirement for individual sarcoglycans and dystrophin in the assembly and function of the dystrophin-glycoprotein complex. *J. Cell Sci.* **113**(Pt. 14), 2535–2544
28. Nowak, K. J., Sewry, C. A., Navarro, C., Squier, W., Reina, C., Ricoy, J. R., Jayawant, S. S., Childs, A. M., Dobbie, J. A., Appleton, R. E., Mountford, R. C., Walker, K. R., Clement, S., Barois, A., Muntoni, F., Romero, N. B., and Laing, N. G. (2007) Nemaline myopathy caused by absence of alpha-skeletal muscle actin. *Ann. Neurol.* **61,** 175–184
29. Beall, C. J., Sepanski, M. A., and Fyrberg, E. A. (1989) Genetic dissection of Drosophila myofibril formation: effects of actin and myosin heavy chain null alleles. *Genes Dev.* **3,** 131–140
30. Palermo, J., Gulick, J., Colbert, M., Fewell, J., and Robbins, J. (1996) Transgenic remodeling of the contractile apparatus in the mammalian heart. *Circ. Res.* **78,** 504–509
31. Kumar, A., Crawford, K., Flick, R., Klevitsky, R., Lorenz, J. N., Bove, K. E., Robbins, J., and Lessard, J. L. (2004) Transgenic overexpression of cardiac actin in the mouse heart suggests coregulation of cardiac, skeletal and vascular actin expression. *Transgenic Res.* **13,** 531–540
32. Marco-Ferreres, R., Arredondo, J. J., Fraile, B., and Cervera, M. (2005) Overexpression of troponin T in *Drosophila* muscles causes a decrease in the levels of thin-filament proteins. *Biochem. J.* **386,** 145–152
33. Suzuki, H., Komiyama, M., Konno, A., and Shimada, Y. (1998) Exchangeability of actin in cardiac myocytes and fibroblasts as determined by fluorescence photobleaching recovery. *Tissue Cell* **30,** 274–280
34. McKenna, N., Meigs, J. B., and Wang, Y. L. (1985) Identical distribution of fluorescently labeled brain and muscle actins in living cardiac fibroblasts and myocytes. *J. Cell Biol.* **100,** 292–296
35. Fyrberg, E. A., Fyrberg, C. C., Biggs, J. R., Saville, D., Beall, C. J., and Ketchum, A. (1998) Functional nonequivalence of *Drosophila* actin isoforms. *Biochem. Genet.* **36,** 271–287
36. Nowak, K., Ravenscroft, G., Jackaman, C., Lim, E., Squire, S., Potter, A., Fisher, R., Morling, P., Griffiths, L., Papadimitriou, J., Sewry, C., Fabian, V., Lessard, J., Crawford, K., Bakker, A., Davies, K., and Laing, N. G. (2007) Transgenic expression of cardiac actin rescues skeletal actin null mice. *Neuromuscul. Disord.* **17**
37. Kumar, A., Crawford, K., Close, L., Madison, M., Lorenz, J., Doetschman, T., Pawlowski, S., Duffy, J., Neumann, J., Robbins, J., Boivin, G. P., O'Toole, B. A., and Lessard, J. L. (1997) Rescue of cardiac alpha-actin-deficient mice by enteric smooth muscle gamma-actin. *Proc. Natl. Acad. Sci. U. S. A.* **94,** 4406–4411
38. Hewett, T. E., Grupp, I. L., Grupp, G., and Robbins, J. (1994) Alpha-skeletal actin is associated with increased contractility in the mouse heart. *Circ. Res.* **74,** 740–746
39. Gordon, D. J., Boyer, J. L., and Korn, E. D. (1977) Comparative biochemistry of non-muscle actins. *J. Biol. Chem.* **252,** 8300–8309
40. Prochniewicz, E., and Strzelecka-Golaszewska, H. (1980) Chicken-gizzard actin. Interaction with skeletal-muscle myosin. *Eur. J. Biochem.* **106,** 305–312
41. Mossakowska, M., and Strzelecka-Golaszewska, H. (1985) Identification of amino acid substitutions differentiating actin isoforms in their interaction with myosin. *Eur. J. Biochem.* **153,** 373–381
42. Prochniewicz, E., and Thomas, D. D. (1999) Differences in structural dynamics of muscle and yeast actin accompany differences in functional interactions with myosin. *Biochemistry* **38,** 14860–14867

Received for publication January 13, 2009.
Accepted for publication February 12, 2009.